Improvement and Evaluation of a Parameterization Scheme for Assessing Dust Devils as Dust Emission in the Northern Margin of the Taklimakan Desert

Mingjie Ma (mmj315@126.com)
Institute of Desert Meteorology
Xinghua Yang
Institute of Desert Meteorology
Qing He
Institute of Desert Meteorology
Ali Mamtimin
Institute of Desert Meteorology

Research Article

Keywords: Taklimakan Desert, Dust devils, Parametric improvement, Dust emission

Posted Date: January 12th, 2022

DOI: https://doi.org/10.21203/rs.3.rs-1130283/v1

[1]Improvement and evaluation of a parameterization scheme for assessing dust devils as dust emission in the northern margin of the Taklimakan Desert

Mingjie Ma, Xinghua Yang*, Qing He , Ali Mamtimin

Abstract: Based on meteorological and dust devil intensification observation data in the desert transition zone of the Xiaotang region in the northern margin of the Taklimakan Desert, and combined with GPS sounding in the hinterland of the Taklimakan Desert, this study investigated the improvement and evaluation of the dust devil parameterization scheme. The results indicate that the thermodynamic efficiency of dust devils after improvement was significantly higher than that before improvement, improving the values by 84.7%, 63.9%, 25.6%, 13.3%, 12.5%, 22.7%, 26.6%, 26.9%, and 21.4% for the hourly intervals from 09:00–17:00, respectively. The annual occurrence of dust devils after improvement was 431 times, 55.2% more than before improvement. The correlation coefficients of convective boundary layer height after improvement was 0.96, higher than that before improvement (0.908). After the improvement, the total annual dust emission time was 181.3 h, 95.9% less than that calculated using the day length before improvement, and 31.8% more than that calculated using sunshine time before improvement. After the improvement, the average vertical dust flux of a single dust devil was 0.25 m^2/s, 68.8% less than that before improvement. After the improvement, the average annual dust emission from dust devils per square kilometer was 15.3 t/km^2, significantly lower than the value of 320.5 t/km^2 before the improvement, approximately one-twentieth of the value.

Keywords: Taklimakan Desert; Dust devils; Parametric improvement; Dust emission

* ✉Xinghua Yang yxhidm@126.com

Institute of Desert Meteorology/Taklimakan Desert Meteorology Field Experiment Station, China Meteorological Administration, Urumqi 830002, China

1 Introduction

Dust aerosols are the most important component of tropospheric aerosols, as they have a significant impact on atmospheric circulation patterns and the Earth's system (Han et al. 2008; Huneeus et al, 2011; Shao et al, 2011a; Jemmett-Smith et al., 2015). The amount of dust emitted affects the Earth's system through many physical, chemical, and biological processes. For example, dust aerosols can directly affect the radiation energy budget of the Earth–air system by scattering and absorbing solar radiation and surface long-wave radiation, resulting in direct climate effects. Dust aerosols can also affect the optical characteristics of clouds and fog as they are a form of condensation nuclei, resulting in indirect climate effects. Dust aerosols play another critical role, in that their long-distance transport drives the global biogeochemical cycle. In that process, dust aerosols are sucked into the atmosphere and transported over long distances along with the high-altitude airflow and delivered to the downstream land and marine areas, bringing a large number of nutrients and trace elements to marine areas and affecting the air-sea carbon exchange (Shao et al., 2011a; Creamean et al., 2013). In addition, dust aerosols can reduce visibility, endanger human health, as well as industrial and agricultural activities, and cause serious property damage (Morman and Plumlee, 2013).

As an important part of the dust cycle, the dust emission process directly determines the number of soil particles that can be released into the atmosphere from the surface. Its critical variables involve a variety of influencing factors, including meteorological factors such as wind speed and direction (Bacon et al., 2011), air temperature and humidity (Park et al., 2011), and soil factors such as soil texture (Alfaro, 2008), soil moisture (Sharratt and Vaddella, 2012), surface roughness (Sharratt and Vaddella, 2014), and soil particle size (Gillette et al., 1980). Wind speed is the most important dynamic condition for dust emission, with gales ($\geqslant$17.0 m/s) being especially important for driving large-scale

43 emissions (Bagnold, 1941). Therefore, it is currently believed that atmospheric dust aerosols are mainly
44 sourced from gale-induced dusty weather processes, such as sandstorms and blowing sand. The
45 amount of dust emitted for dusty weather processes is typically very large, matching the observed
46 aerosol indices such as PM10 and PM2.5, as well as sedimentation and satellite observations among
47 corresponding periods. However, dusty weather processes have low frequency, owing to the high
48 amount of sunny days without sandstorms. If only dusty weather processes are considered, there would
49 be much less dust aerosol, yet the observed aerosol index is still relatively high. This means that other
50 mechanisms of dust aerosol emissions must exist (Han et al., 2008; Huang et al., 2008; Deng et al.,
51 2009; Han et al., 2016). Among the possible mechanisms, dust devils are considered to be an important
52 example (Han et al., 2008). The formation of dust devils can be described as follows. In sunny,
53 breezeless, or breeze conditions, strong solar radiation increases the sensible heat flux on the ground
54 surface, which in turn causes the air temperature near the ground surface to gradually increase. In the
55 convective boundary layer, owing to thermal buoyancy, the hot air forms thermal convection (Deng et
56 al., 2011), which in turn forms the dust devil (Figure 1).

57 Studies have reported that dust devils are important contributors to atmospheric dust. Dust devils
58 contributed an annual total emission of approximately 215×10^7 t of dust aerosols, which accounted for
59 approximately 34±19% of global total emissions (Koch and Renno, 2005). The contribution of dust
60 devils to dust aerosols is approximately 53% in the Taklimakan Desert in northwest China (Han et al.,
61 2016), approximately 65% in the continental U.S., and more than 30% in the Sahara Desert (Marsham
62 et al., 2008). Based on the above considerations, the contribution of dust devils to atmospheric dust
63 aerosols cannot be ignored.

The Taklimakan Desert is a major source of dust in East Asia. However, the research on dust aerosol emissions in this region mainly focuses on emissions from dusty weather without considering the contributions of dust devils to regional dust aerosol emissions (Zhang et al, 1997; Chen et al, 2016; Liu et al, 2016; Meng et al, 2019). As a result, there may be a huge underestimation of dust aerosols. Therefore, to investigate the contribution of dust aerosols from dust devils in the Takliman Desert, the Xiaotang region, located at the northern margin of the Taklimakan Desert, was selected as the study area. Using a combination of enhanced observation data of dust devils and meteorology data, combined with global positioning system (GPS) sounding data in the Tazhong area in the hinterland of the desert, some key variables in the original parameterization scheme for dust devils to dust emissions have been improved. The improved variables include the convection boundary layer height, thermodynamic efficiency, and average vertical dust flux of a single dust devil. The improved parameterization scheme was used to determine the number of dust devil occurrences, dust emission time, and dust emission research in the study area. Further, the original dust emission parameterization scheme and the measured data were comparatively analyzed to provide additional support for the research on Taklimakan Desert dust aerosol emissions transmission. To a large extent, the findings of this study contribute to compensating for the lack of the amount of dust emitted in global dust simulations; moreover, the results represent a re-evaluation of the overall climate effect of dust aerosols.

2. Data and Methods

2.1 Study area

The Xiaotang region is located at the northern margin of the Taklimakan Desert in northwest China (Fig. 1). The underlying soil is mainly composed of fine (125–250 μm) and very fine (62.5–125 μm) sand (Yang et al, 2012), and ancient riverbeds are exposed in some areas (He et al, 2011). This region

has a long sunshine duration and strong solar radiation. The annual statistics are as follows: average temperature of 12.4 °C, average wind velocity of 2.5 m/s, and average precipitation of 15.2 mm. Therefore, the frequency of dusty weather occurrences in this region is extremely high; sandstorms and dust devils occur throughout the year. Statistically, the annual average number of sandstorm occurrence days has been found to be 42 (Yang et al, 2012), with most occurring in spring and summer, and one example in 1994 where a sandstorm lasted for 71 days. Suitable climatic conditions are also conducive to the formation of dust devils. According to meteorological station observation records, dust devils have been observed in the Xiaotang region throughout the year, with the frequency being highest from June to September. For these reasons, this region was selected as the study area for the observation of dust wind.

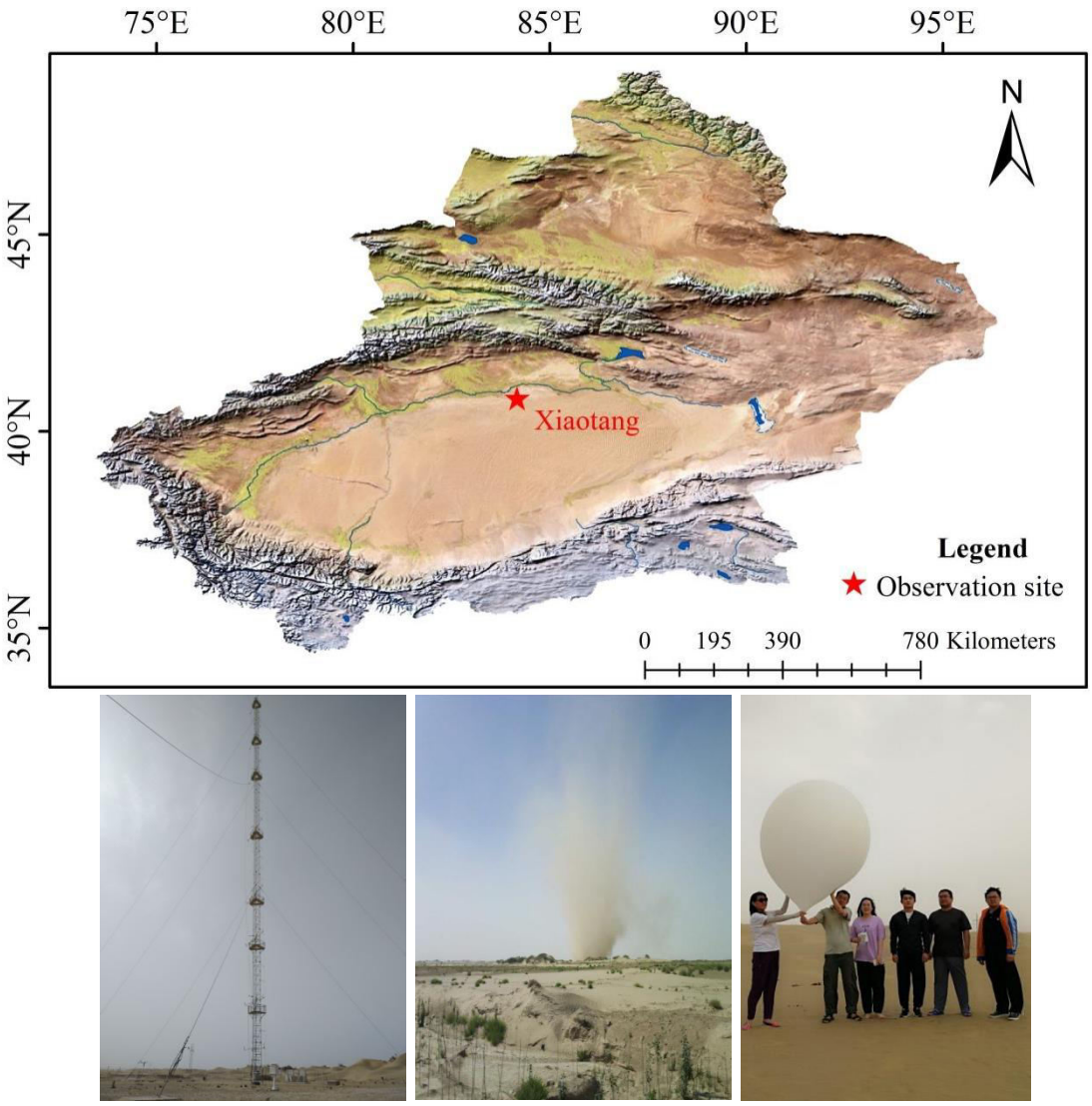

Fig. 1 Location of the test site (Xiaotang located at the northern margin of the Taklimakan Desert), meteorological observation tower, dust devil, and GPS sounding equipment

2.2 Meteorological elements and observations of dust devils

A 100-m gradient detection platform was used to observe the near-surface micrometeorology. The platform was equipped to measure five levels (0.5, 1.0, 2.0, 4.0, 10.0, 20, 32, 47, 63, 80 ,100 m) of gradient wind velocities (Metone 010C) and wind direction (Metone 020C). Additional sensors were used to measure the air temperature and humidity (Vaisala HMP45C), and a pressure sensor (Vaisala PTB220) was installed at a height of 1.0 m. Soil observations included soil temperature and humidity. Probes for measuring soil temperature (Campbell 109 L) were separately buried at depths of 0, 5, 10, 20, and 40 cm; those for measuring soil moisture (Campbell CS616) were separately buried at depths

of 1.5, 5.0, and 10.0 cm. The solar radiation observation instrument, model number CNR-1, was manufactured by Kipp and Zonen, Netherlands. The measurement data of all sensors were stored in the CR1000 data collector (Campbell), which could provide measurement data at various time steps including 1s, 1 min, 30 min, and 1 h. All data used in this study were average minute data based on the local time (note that the time difference between Xiaotang and Beijing is 2 h, 22 min, 48 s).

Continuous observations of dust devils were carried out over two periods: from July 6–14, 2014, and August 6–28, 2018. The daily observation duration was 9:00–17:00 (local time). The frequency of occurrence and duration of each occurrence were observed and recorded, yielding a total of 130 occurrences.

2.3 Calculation of dust emission amounts by dust devils

Renno et al. (1998) proposed the original dust devil thermodynamic equation based on observations and experiments. The equation is the first definition of the thermodynamic efficiency η of a dust devil and can be used to determine the scale, vortex strength, and core pressure of the dust devil (Koch and Renno, 2005):

$$\eta = \frac{\Gamma_{ad} Z_{CBL}}{T_s}, \quad (1)$$

where Z_{CBL} is the height of the convective boundary layer (m), T_s is the surface temperature (°C), and Γ_{ad} is the adiabatic lapse rate, a nondimensional coefficient. The present study utilized the fitted equation of the hourly average convective boundary layer height and hourly average surface temperature determined by GPS sounding in the hinterland of the Taklimakan Desert in July 2017 located 200 km from the study area. Because the atmospheric water vapor in the desert was very small, the adiabatic lapse rate was considered to be constant (10 K/km).

Renno and Ingersoll (1996) provided the effective area of a dust devil as:

$$S=S_T\sigma \quad (2)$$

where S_T is the total area of the dust devil (the present study area centered at the Xiaotang land–atmosphere interaction observation station, extending 1 km from east to west and from north to south, covering an area of 1 km^2), and σ is the ratio of the effective dust emission area (Renno and Ingersoll, 1996), which is calculated as:

$$\sigma = \left(\frac{\mu}{\eta}\right)^{1/2}\left(\frac{\mathrm{V}P}{\rho_{air} g T_R}\right)^{3/2}\left(\frac{F_{in}}{\rho_{air}}\right)^{-1/2} \quad (3)$$

where μ is a dimensionless mechanical energy friction loss coefficient (ranging from to 12–24, with an average value of 18 in this study); ΔP is the pressure difference between the ground surface and the top of the convective boundary layer ($\Delta P=\rho_{air} g Z_{CBL}$), ρ_{air} is the air density (1.0 kg/m^3), g is the gravitational acceleration (9.8 m/s^2), F_{in} is the heat flow that drives the dust devil (11±5 kW/m^2, with an average value of 11 kW/m^2 in the present study), and T_R is the effective solar radiation time scale of the convective boundary layer (9 ×10^5 s) (Koch and Renno, 2005).

The amount of dust emitted by a dust devil can be determined using the following equation (Koch and Renno, 2005):

$$F_{tot} = PDDP_{hours} \times S \times F_d \quad (4)$$

where F_{tot} is the total amount of dust particles (g) transported into the air by the dust devil; $PDDP_{hours}$ is the potential total number of hours of dust devil events per year, and F_d is the dust flux of the dust devil. The average vertical dust flux of a single dust devil in the study area was 0.25 g/(m^2·s), and the maximum and minimum dust fluxes were 0.4 and 0.1 g/(m^2·s), respectively (Luan and Han, 2016; Liu and Zhao, 2016).

3 Results and Discussion

3.1 Improvement of the thermodynamic efficiency of dust devils

According to Eq. (1), the thermodynamic efficiency of the dust devils is a function of the convective boundary layer height and surface temperature. In previous studies, the daily variation in the thermodynamic efficiency of dust devils has been calculated using the convective boundary layer height and surface temperature observed on sunny days in the Gobi Desert in Dunhuang, during the summer from May 29 to June 9, 2000 (Fig. 3) (Duan et al, 2013). Moreover, in previous studies, the monthly variation of the thermodynamic efficiency of dust devils has been calculated using the convective boundary layer height (fitting with month) (Eq. 5) (Liu et al, 2008; Marsham et al, 2008; Qiao et al., 2010; Li et al, 2011) and the surface temperature observed in the surrounding area of the Taklimakan Desert (Fig. 4) (Duan et al, 2013). However, owing to the particularity of the region and the lack of data, errors were inevitable in those calculation results. Therefore, the thermodynamic efficiency of dust devils was improved in this study. To do this, the thermodynamic efficiency of dust devils in the Xiaotang area was calculated using the measured convective boundary layer height of the Taklimakan Desert (based on July 2017 GPS sounding observation data of the hourly average convection boundary layer height in the desert's hinterland) and surface temperature data (based on the average surface temperature fitting equation, Eq. 6). The results are shown in Tables 1 and 2. Equation (5) is given as:

$$Z_{CBL}=-100.7M^2+1316M-536.4 \quad (5)$$

where ZCBL is the convective boundary layer height and M is the month. The correlation coefficients (r) between the fitted and observed values of these parameters were 0.90, respectively ($p < 0.01$). Equation (6) is given as:

$$\begin{cases} Z_{CBL} = 221.7T_s - 6769.9 & (x \geq 32) \\ Z_{CBL} = 9.89T_s - 13.6 & (x < 32) \end{cases} \quad (6)$$

where ZCBL is the convective boundary layer height, and T_s is the surface temperature. The correlation coefficients (r) between the fitted values and the observed values of these parameters were 0.95 and

0.97, respectively ($p < 0.01$). Compared with the convective boundary layer height fitted by month in Eq. (5), the convective boundary layer height fitted by surface temperature (Eq. 6) in this study has a higher fitting coefficient and a more significant fitting effect (0.96 > 0.90). Therefore, the daily and monthly variations in the thermodynamic efficiency of dust devils in the Xiaotang region were calculated using Eqs. (1) and (6), respectively. Figures 2 and 3 compare the improved thermodynamic efficiency of the dust devils with that before the improvement.

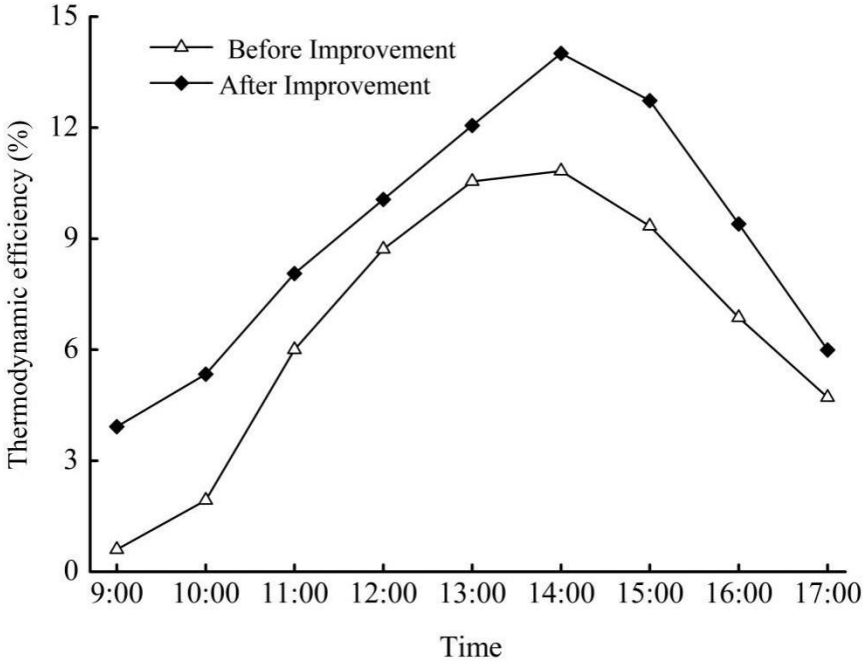

Fig. 2 Diurnal variations in the thermodynamic efficiency of dust devils.

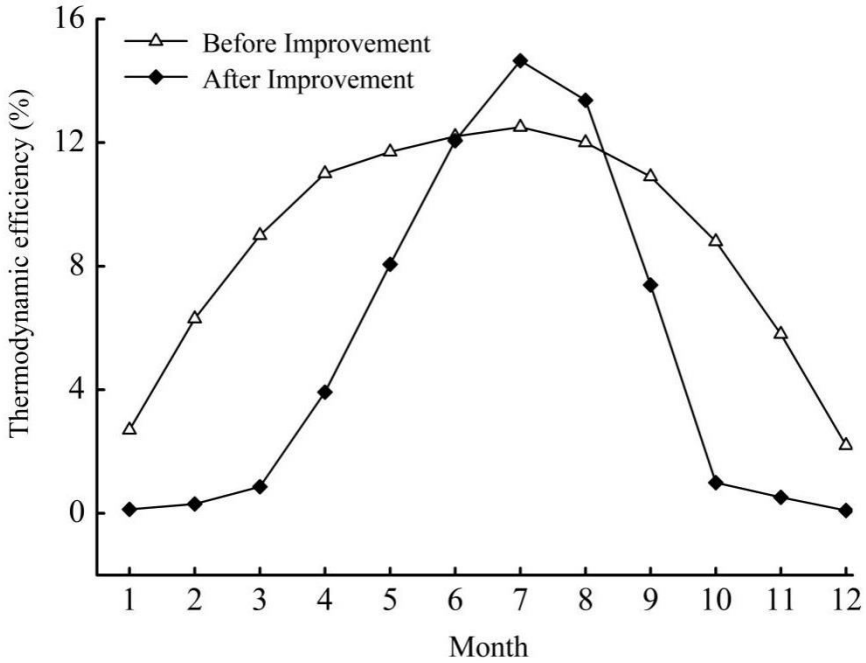

Fig. 3 Monthly variations in the thermodynamic efficiency of dust devils. The observed data before improvement was taken from previous studies (Liu et al, 2008; Qiao et al, 2010; Li et al, 2011; Duan et al, 2013).

As can be seen from Figure 2, the thermodynamic efficiency of the dust devils after improvement was significantly higher than that before improvement, returning values that were 84.7%, 63.9%, 25.6%, 13.3%, 12.5%, 22.7%, 26.6%, 26.9%, and 21.4% higher than those before improvement for 09:00–17:00, respectively. In addition, the daily variation in the thermodynamic efficiency of dust devils before and after the improvement showed a single-peak distribution, which increased starting at 09:00 and peaked at 14:00, and then showed a significant downward trend. As shown in Figure 3, the monthly variation in the thermodynamic efficiency of dust devils before and after improvement shows a seasonal variation pattern: summer > spring > autumn > winter. The thermodynamic efficiency of the dust devils before improvement increased rapidly from January in winter, reaching a peak of 12.5% in July in summer, then showed a significant downward trend, and decreased to the minimum value of 2.2% in December, with a difference of approximately 5.6 times between the maximum and minimum values. The thermodynamic efficiency of the dust devils after improvement was small from January to March (less than 1%) and grew slowly. It then grew rapidly from March and reached a peak of 14.6% in July, and then showed a significant downward trend from July to October, a slow downward trend from October to December, and a decrease to the minimum value of 0.09% in December. The increase or decrease in the thermodynamic efficiency of dust devils from April to September after the improvement was greater than that before the improvement, which may be related to the fact that the surface specific heat capacity of sand particles in Xiaotang is smaller than that of the Gobi Desert; moreover, the solar radiation is stronger in spring and summer, surface temperature rises faster, convective turbulence is stronger, and convective boundary layer height is higher (Liu et al, 2008; Marsham et al, 2008; Qiao et al, 2010; Li et al, 2011).

3.2 Improvement of frequency evaluation of dust devils

Figure 4 shows the daily variation of dust devil occurrence times before the improvement (based on data of a meteorological station at Peacock River in the southern part of the Xinjiang region) and after the improvement (based on data of this study). As can be seen from the figure, the occurrence times of dust devils before and after the improvement showed a single-peak distribution, which first appeared at 09:00, and almost no dust devils were observed after 18:00. The occurrence of dust devils

after the improvement was three, two, and four times more than before improvement, at 9:00–10:00, 16:00–17:00, and 17:00–18:00, respectively. The occurrence of dust devils before the improvement was 2, 8, 13, 26, 22, and 2 times higher than that after improvement, at 10:00–11:00, 11:00–12:00, 12:00–13:00, 13:00–14:00, 14:00–15:00, and 15:00–16:00, respectively. In addition, the peak values of the dust devils before improvement occurred 47 times, during 13:00–14:00 and 14:00–15:00, accounting for 24.4% of the total number of times. The peak values of the dust devils after improvement only occurred 25 times during 14:00–15:00, accounting for 19.8% of the total number of times, 22 times less than before.

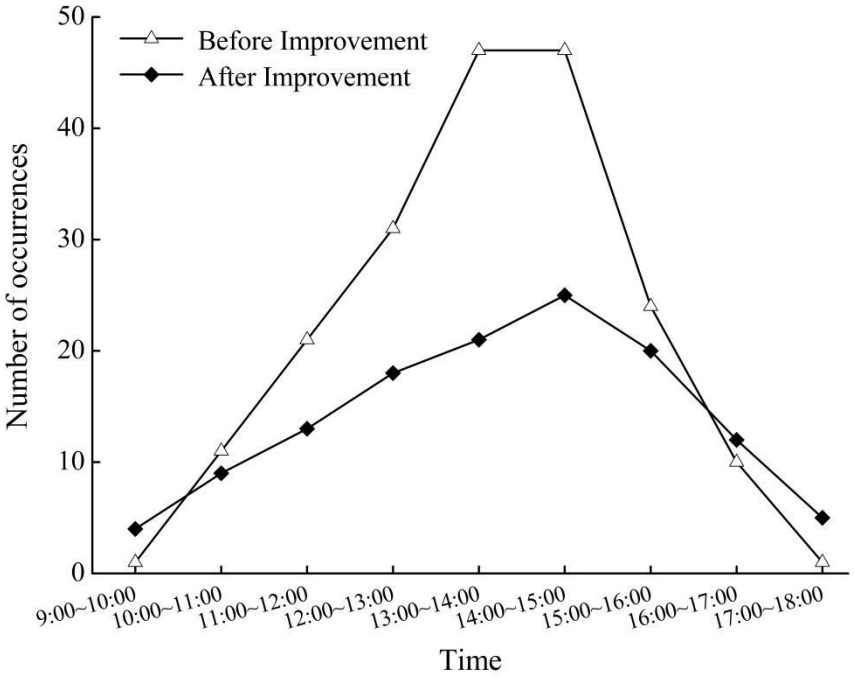

Fig 4. Diurnal occurrence of dust devils. The data before improvement were obtained from Yue, 1983 and Duan et al., 2013; the data after improvement are the measured data in the Xiaotang region from this study.

Based on the above analysis of the thermodynamic efficiency characteristics of dust devils, it was found that the variation characteristics of the thermodynamic efficiency of dust devils were basically consistent with the measured number of dust devil daily occurrence in this study, indicating that the improved formula can better reflect the variation characteristics of the real number of dust devils. Based on this, this study used the thermodynamic efficiency and frequency of dust devils to fit the monthly variation of the frequency of dust devils (Fig. 5). The resultant fitting equation was Y

=1.43X+0.62, where X represents the thermodynamic efficiency of dust devils and Y represents the occurrence times of dust devils. The correlation coefficient (r) between the fitted values and the observed values of these parameters was 0.92 ($p < 0.01$).

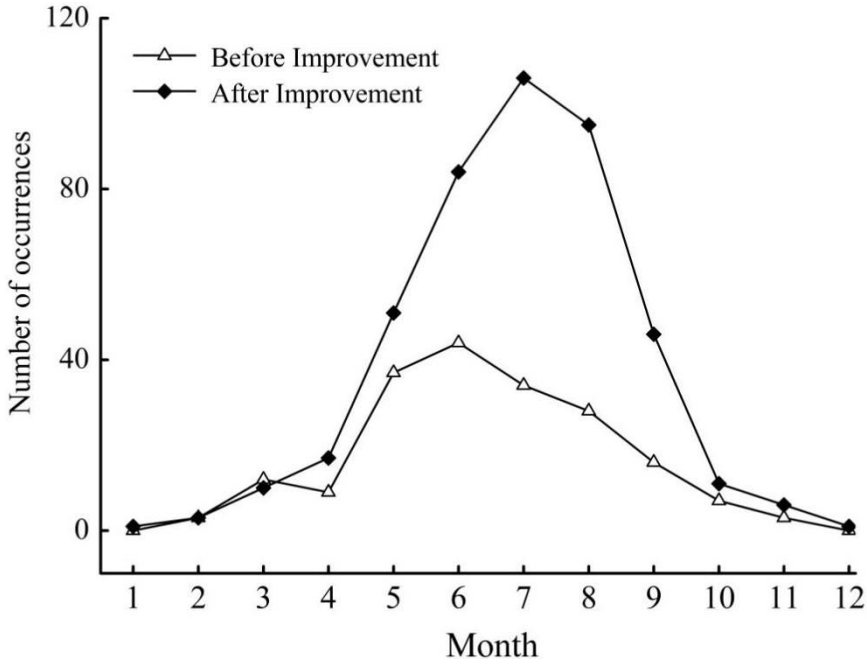

Fig. 5 Monthly variations in the occurrence of dust devils.

As shown in Figure 5, the monthly variation in the occurrence frequency of the dust devils before improvement showed a seasonal distribution pattern: summer (106 times) > spring (58 times) > autumn (26 times) > winter (3 times), and the total annual occurrence frequency was 193 times. The monthly variation in the occurrence frequency of the dust devils after improvement also showed a seasonal distribution pattern: summer (285 times) > spring (78 times) > autumn (63 times) > winter (5 times), and the total annual frequency of dust devils was 431. Thus, the frequency of dust devils after improvement was 2.2 times higher than that before improvement. After improvement, the monthly peak value of dust devils occurred in June with 44 times, and the monthly peak value of dust devils occurred in July with 106 times, about 2.4 times of that before the improvement. This may be due to the fact that the Xiaotang region belongs to the desert transition zone, and so would have increasing surface roughness of the p

articles. A small increase in surface roughness not only increases the vortex scale but also reduces the speed threshold for transporting fine particles to the upper air, thus picking up more dust particles and facilitating the occurrence of dust devils (Luan et al, 2016). In addition, for the values after improvement, it was found that in sunny, calm, or weak wind conditions in summer, the occurrence of dust devils was higher (431 times), while the occurrence of dust wind before improvement was less (193 times). Overall, the findings indicate that the assessment of the occurrence of dust wind has been improved with the method in this study.

Tab. 1 Temporal variation in the thermodynamic efficiency of dust devils

Time	Z_{CBL}(m)	Solar radiation (W/m^2)	T_s (°C)
09:00	1210	290	36
10:00	1660	350	38
11:00	2540	420	42
12:00	3200	470	45
13:00	3870	500	48
14:00	4540	440	51
15:00	4100	390	49
16:00	2980	350	44
17:00	1870	260	39

Tab. 2 Monthly thermodynamic efficiency variations of dust devils

Month	Z_{CBL}(m)	Solar radiation (10^6J/m^2)	T_s (°C)
1	36	220	5
2	86	350	10
3	260	530	28
4	1210	600	36
5	2540	720	42
6	3870	760	48
7	4760	770	52
8	4320	630	50
9	2320	520	41
10	300	430	31
11	150	300	16
12	27	210	4

3.3 Improvement of the dust emission time observations of dust devils

Table 3 shows the enhanced observations of dust devil duration in the Xiaotang region. The

observation results show that the duration of dust devils was generally short; 72.5% of dust wind duration was less than 10 min, and 10–20 min only accounted for 27.5% of the total time. In this study, the dust emission time of dust devil months was obtained by multiplying the number of dust devil months by the measured duration of dust devils and the number of sunny days and breeze days in that month. The background weather data (rain days, cloudy days (total cloud cover > 70%), windy days (wind speed≥ 5 m/s), sand blowing, and sandstorm weather that are not conducive to the occurrence of dust devils were eliminated. Thus, the dust devil annual dust emission time was improved (as described in the previous paragraph, previous authors respectively used the day length (Duan et al, 2013) and sunshine duration (Luo et al, 2017) to replace the dust wind annual dust emission time). Overall, the accuracy and effectiveness of the data were improved, as shown in Figure 6.

Tab. 3 Duration of dust devils

Duration (min)	1.1–4.0	4.1–7.0	7.1–10.0	10.1–13.0	13.1–16.0	16.1–20.0
Number	50	28	20	16	13	8
Percentage (%)	37	20.7	14.8	11.9	9.7	5.9

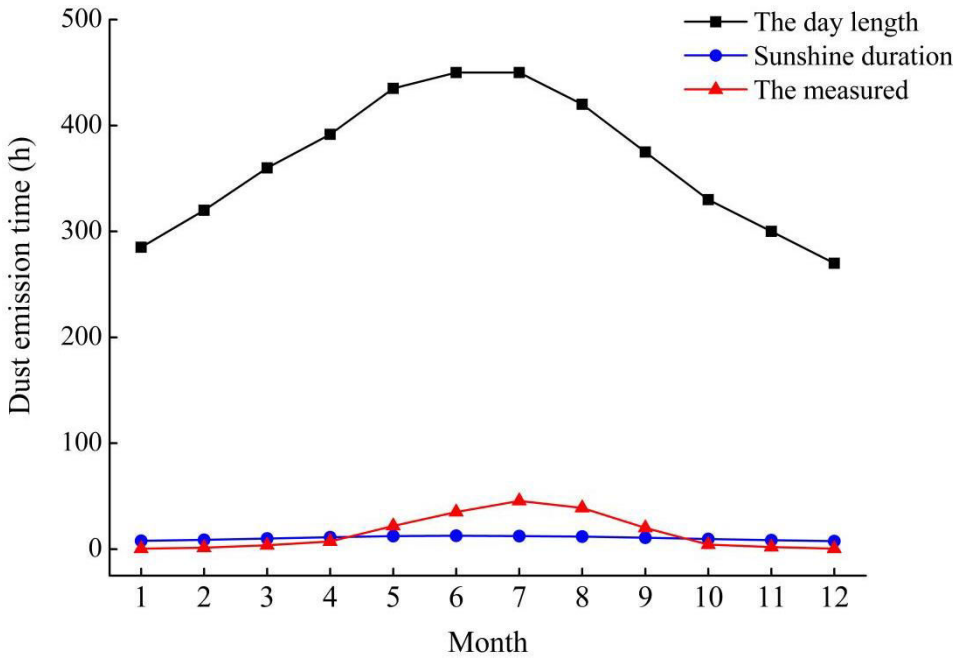

Fig. 6 Dust emission time of dust devils.

Figure 6 shows that the measured dust devils dust emission time (181.3 h) in this study is lower than that calculated using the day length (4386.7 h) and higher than that calculated using the sunshine duration (123.8 h). From January to December, the measured dust emission time of dust devils was 99.8%, 99.5%, 99.0%, 98.1%, 95.0%, 92.2%, 89.9%, 90.7%, 94.6%, 98.7%, 99.3%, and 99.8% less, respectively, than that calculated using the day length; furthermore, from May to September, the measured dust devils dust emission time was 43.5%, 63.8%, 72.9%, 69.2%, and 46.1% more, respectively, than that calculated using the sunshine time. In addition, the measured dust devils dust emission time, day length, and sunshine duration in this study all showed the same seasonal distribution pattern, with an increase in spring, a peak in summer, and a significant decrease in autumn and winter.

3.4 Improvement of the assessment of dust emission from dust devils

Figure 7 shows the annual average, maximum, and minimum dust emissions from dust devils before and after improvement. As can be seen from the figure, the average annual dust emission from dust devils before and after the improvement presents a significant seasonal distribution pattern: summer > spring > autumn > winter. The average annual dust emission from dust devils per square kilometer after the improvement was 15.3 t/km^2, and that before the improvement was 320.5 t/km; thus, the improved value is significantly smaller, approximately one-twentieth of that value. In addition, before the improvement, the average annual dust emission from dust devils began to increase from January, reaching a peak of 44.7 t/km in July, then showing a downward trend, and decreasing to a minimum of 5.6 t/km in December. Before the improvement, the seasonal pattern was: summer (127.4 t/km^2) > spring (95.1 t/km^2) > autumn (66.6 t/km^2) > winter (31.4 t/km^2). After the improvement, the average annual dust emission was small from January to April, less than 0.2 t/km^2, and grew slowly. It increased rapidly from May and reached a peak of 5.26 t/km in July, then showed a significant downward trend from August to October and slowly declined from October to December. After the improvement, the seasonal pattern was: summer (12.6 t/km^2) > spring (1.5 t/km^2) > autumn (1.2 t/km^2) > winter (0.3×10^{-2} t/km^2), and the range of increase and decrease from April to September were both larger than before. This may be related to the selection of parameters in the parameterization scheme of dust devils (Eq. 4).

The improvements to the parameterization scheme for dust devils to dust emissions in this study can be described as follows. First, the thermodynamic efficiency of dust devils was

improved by using recalculated convective boundary layer height and surface temperature data. Second, the number of dust devils was improved by fitting the number of measured daily dust devils in the Xiaotang region with the new thermodynamic efficiency. Third, the average vertical dust flux of dust devils was improved by calculating the flux of single dust devils in the Xiaotang region using dust devil opacity and an empirical formula (Liu et al, 2016; Luan et al, 2016). Finally, the dust devil dust emission time was improved by obtaining the total number of hours of dust devil events per year through multiplying the number of dust devil months by the measured duration of dust devils and the number of sunny and breezy days in that month. Through these improvements of the parameterization scheme, the amount of dust emitted by a dust devil calculated in this study is more effective and reliable.

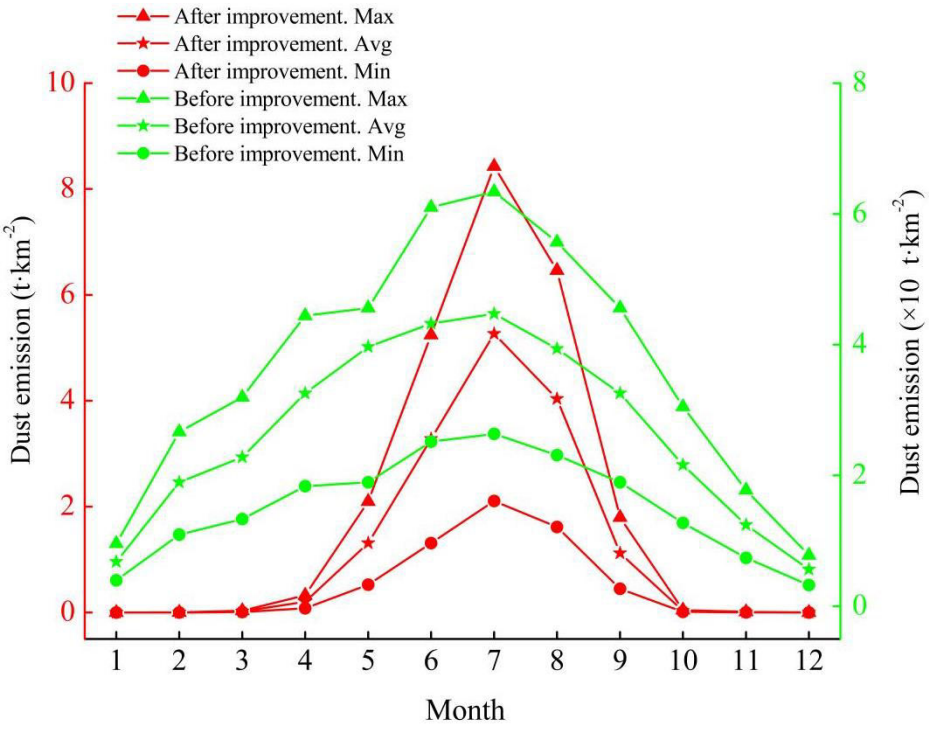

Fig. 7 Dust emission amount of dust devils in the Taklimakan Desert.

4 Conclusions

Based on meteorological observation data of dust devils over the desert transition zone at the northern margin of the Taklimakan Desert and GPS sounding data in the desert's hinterland, this study improved the parameterization scheme evaluation for calculating dust emission from dust devil occurrence. The following conclusions were obtained:

(1) The daily variation in the thermodynamic efficiency of the dust devils after improvement showed a single-peak distribution, which increased starting at 09:00 and peaked at 14:00, and then

showed a significant downward trend. From 09:00 to 17:00, the thermodynamic efficiency of dust devils after improvement was increased by 84.7%, 63.9%, 25.6%, 13.3%, 12.5%, 22.7%, 26.6%, 26.9%, and 21.4%, respectively, for the nine hourly intervals.

(2) After improvement, the number of dust devil days showed a significant single-peak distribution, with the daily occurrence of dust devils beginning at 09:00, while almost no dust wind was observed after 18:00. The peak appeared between 14:00 and 15:00, accounting for 19.7% of the total occurrence times. In addition, the duration of dust devils was generally short; 72.5% lasted for less than 10 min, 21.6% lasted 10–16 min, and only 5.9% lasted for more than 16 min.

(3) The interannual amount of dust emitted by a dust devil per square kilometer in the study area showed a significant seasonal distribution: summer (12.6 t/km^2) > spring (1.5 t/km^2) > autumn (1.2 t/km^2) > winter (0.3×10^{-2} t/km^2), accounting for 82.3%, 9.8%, 7.8%, and 0.1% of the annual amounts of dust emitted, respectively. The total annual sediment load for the improved dust wind was 15.3 t/km. The total amount of dust emitted by a dust devil before improvement was 320.5 t/km, and was 15.3 t/km after the improvement, about one-twentieth of the previous value.

Statements and Declarations

Conflict of interests: All authors declare they have no financial interests

Funding Statement: This work was supported by the Project of Desert Meteorological Science Research Foundation of China (grant number Sqj2020001) and Tianshan Youth Talents Plan Project of Xinjiang (grant number 2018Q040). Author Mingjie Ma has received research support from “Institute of Desert Meteorology, China Meteorological Administration, Urumqi 830002, China”

Author Contributions: All authors contributed to the study conception and design. Material preparation, data collection and analysis were performed by Xinghua Yang, Qing He, and Ali Mamtimin. The first draft of the manuscript was written by Mingjie Ma, and all authors commented on previous versions of the manuscript. All authors read and approved the final manuscript.

Availability of data and material: The datasets generated during and/or analysed during the current study are not publicly available due to relevant regulations of the company but are available from the corresponding author on reasonable request

Data transparency: Authors promise that all data and materials as well as software application or custom code support their published claims and comply with field standards.

Code availability: The Paper code is available

Ethics approval: Authors promise that the work (figures, tables, or text passages) described has not been published before; that it is not under consideration for publication anywhere else; that its publication has been approved by all co-authors. The results should be presented clearly, honestly, and without fabrication, falsification or inappropriate data manipulation (including image based manipulation).

Consent to participate: This article is supported and participated by all authors

Consent to publication： This article is published with the permission of the company and all authors

References

Alfaro SC (2008) Influence of soil texture on the binding energies of fine mineral dust particles potentially released by wind erosion. Geomorphology 93: 157-167.

Bacon SN, McDonald EV, Amit R, Enzel Y, Crouvi O (2011) Total suspended particulate matter emissions at high friction velocities from desert landforms. Journal of Geophysical Research: Atmospheres 116: F03019.

Bagnold RA．The Physics of Blown Sand and Desert Dunes．London: Methuen and Co，1941: 1-40．

Creamean J M, Suski K J, Rosenfeld D, et al (2013) Dust and Biological Aerosols from the Sahara and Asia Influence Precipitation in the Western U.S., Science 339(6127): 1572-1578

Chen SY, Huang JP, Kang LT, et al (2017) Emission, transport, and radiative effects of mineral dust from the Taklimakan and Gobi Deserts: Comparison of measurements and model results. Atmospheric Chemistry and Physics 17(3): 1-43.

Duan JP, Han YX, Zhao TL (2013) The contribution of dust devils to dust aerosol and its relationship with solar radiation. China Environmental Science 33: 43-48 (In Chinese).

Deng ZQ, Han YX, Bai HZ (2009) Analysis of the causes of changes in dust aerosol content in desert

areas. China Environmental Science 29: 1233-1238 (In Chinese).

Deng ZQ, Han YX, et al (2011) Relationship between dust aerosol and solar radiation in gebi desert in North China. China Environment Science 31(11): 1761-1767.

Gillette DA, Adams J, Endo A, Smith D, and Kihl R (1980) Threshold velocities for input of soil particles into the air by desert soils. Journal of Geophysical Research: Oceans 85(C10): 5621-5630.

He Q, Yang XH, Mamtimin A (2011) Observation and Research on Wind Erosion and Sanding in Taklimakan Desert--Experimental Introduction and Observation Results. Journal of Desert Research 31: 315-322 (In Chinese).

Huneeus N, Schulz M, Balkanski Y, et al (2011) Global dust model intercomparison in AeroCom phase l. Atmospheric Chemistry and Physics 10(10):7781-7816.

Huang J, Patrick M, et al (2008) Long-range transport and vertical structure of Asian dust from CALIPSO and surface measurements during PACDEX. Journal of Geophysical Research Atmospheres 113(D23): 2036-2044.

Han Y, Dai X, Fang X, et al (2008) Dust aerosols: a possible accelerant for an increasingly arid climate in North China. Journal of arid environments 72(8): 1476-1489.

Han Y Wang K Liu F et al (2016) The contribution of dust devils and dusty plumes to the aerosol budget in western China. Atmospheric Environment 126: 21-27.

Jemmett-Smith BC, Marsham JH, Knippertz P, et al (2015) Quantifying global dust devil occurrence from meteorological analyses. Geophysical Research Letters 42(4): 1275-1282.

Koch J, Renno NO (2005) The role of convective plumes and vortices on the global aerosol budget. Geophysical Research Letters 32: 109-127.

403 Liu C, Zhao TL (2016) Observation, parameterization and climate simulation of dust emission
404 processes. Dissertation, Nanjing University of Information Science and Technology. (In
405 Chinese).
406 Liu MX, Zhang HS (2008) The characteristics of the PBL structure and its temporal evolvement during
407 summer and winter over Gobi area. Beijing University. (In Chinese).
408 Li YY, Zhang Q, et al (2011) Relationship between Atmosphere Boundary Layer Characteristics and
409 Sand-dust Weather Climatology in Minqin. Journal of Desert Research 5(31): 757-768. (In
410 Chinese).
411 Luan, ZP, Han, YX (2016) Observing the structure of desert dust devil Taklimakan and large eddy
412 simulation study. Dissertation, Nanjing University of Information Science and Technology (In
413 Chinese).
414 Luan ZP, Zhao TL, Han YX (2016) Progress dust devil in arid and semi-arid areas. Desert and Oasis
415 Meteorology 10: 1-8 (In Chinese).
416 Luo H, Han YX (2017) The temporal evolution of the atmospheric boundary layer in arid regions and
417 the contribution of dust to wind to atmospheric dust aerosols. Dissertation, Nanjing University of
418 Information Science and Technology (In Chinese).
419 Morman SA, Plumlee GS (2013) The role of airborne mineral dusts in human disease. Aeolian
420 Research 9: 203-212.
421 Marsham J, Parker D, Grams C, et al (2008) Observations of mesoscale and boundary-layer scale
422 circulations affecting dust transport and uplift over the Sahara. Atmospheric Chemistry and
423 Physics 8: 6979-6993.
424 Meng L, Yang XH*, Zhao TL, et al (2019) Modeling study on three-dimensional dimensional

425 distribution of dust aerosols during a dust storm over the Tarim Basin, Northwest China.
426 Atmospheric Research 218: 285-295.
427 Park SU, Park MS, Chun YA (2011) Parameterization of dust concentration (PM10) of dust events
428 observed at Erdene in Mongolia using the monitored tower data. Science of the Total Environment
429 409: 2951-2958.
430 Qiao J, Zhang Q, et al (2010) Comparison of Atmospheric Boundary Layer in Winter and Summer
431 over Arid Region of Northwest China. Journal of Desert Research 3(30): 421-429. (In Chinese).
432 Renno NO. Burkett ML, Larkin MP (1998) A Simple Thermodynamical Theory for Dust Devils.[J].
433 Journal of the Atmospheric Sciences 55(21):3244-3252.
434 Renno NO, ingersoll AP (1996) Natural convection as a heat engine: A theory for CAPE. J . Atmos.
435 Sci 53:572-585.
436 Sharratt BS, Vaddella VK (2012) Threshold friction velocity of soils within the Columbia Plateau.
437 Aeolian Research 6: 13-20.
438 Sharratt BS, Vaddella V (2014) Threshold friction velocity of crusted windblown soils in the Columbia
439 Plateau. Aeolian Research 15: 227-234.
440 Shao YP, Wyrwoll KH, Chappell A, Huang JP, Lin ZH, et al (2011a) Dust cycle: An emerging core
441 theme in Earth system science. Aeolian Research 8: 181-204.
442 Yang XH, Li HJ, He Q (2012) Characteristics of Sandstorm Activity in Spring in the Taklimakan
443 Desert Desert Transition Zone: A Case Study of Xiaotang. Journal of Desert Research 32:
444 915-920 (In Chinese).
445 Yue Z (1983) Dust devils on the Gobi Desert in southern Xinjiang. Meteorol. Monthly 4: 33 (in
446 Chinese).

447 Zhang XY, Arimoto R, An Z (1997) Dust emission from chinese desert sources linked to variations in
448 atmospheric circulation. Journal of Geophysical Research 102: 28041-28047.